Retardation Times of Deoxyribonucleic Acid Solutions. II. Improvements in Apparatus and Theory

Lynn C. Klotz* and Bruno H. Zimm

Department of Chemistry (Revelle College), University of California, San Diego, La Jolla, California 92037. *Received March 3, 1972*

ABSTRACT: An improved version is described of an instrument for measuring retardation times of dilute solutions of very large random-coil macromolecules such as DNA in a creep-recovery type of experiment. Retardation times are closely related to molecular weight and size. The relations are derived theoretically using the formulas of the "beads–springs" model. The effects of size heterogeneity on the results are considered. Relations are worked out involving the specific viscosity, the amount of elastic recoil, and the time course of the recoil, and the possible advantages of combining these results with sedimentation measurements are explored. It is concluded that molecular weight can be found from creep-recovery measurements alone if the molecule is known to be a linear random coil, but if there is a possibility of some other structure, such as a circular chain, or if there is much heterogeneity, it is necessary to have sedimentation measurements in addition for an unambiguous determination. Details of construction of the improved version of the instrument, which is based on the Gill–Thompson Cartesian-diver viscometer, are given.

In a previous paper,[1] we described a method for determining the relaxation times of DNA molecules in dilute solution in a creep-recovery experiment. The relaxation time is markedly sensitive to the size of a chain molecule. We have found this method to be uniquely useful in characterizing the size of DNA extracted from bacteria, and we are submitting the results of that study to a biological journal. In the course of this study, however, we have made considerable changes in the apparatus and have had to develop some new theory in order to deal with questions of polydispersity and molecular shape. The present paper reports on these developments.

Experimental Section

The Instrument. The instrument is still basically the rotating Cartesian-diver viscometer described by Gill and Thompson[2] with provision for continuous recording of the rotor angle as a function of time. The changes from the previous description[1] are mainly in the angle-measuring device.

Figure 1 shows a schematic diagram. Unpolarized white light (1) passes through a rotating polarizer (angular velocity $\omega_a/2$), and the now-polarized light (2) is focused on a glass plate. About 15% of the light is reflected (3) through a stationary Polaroid disk so that the light which reaches the photocell (4) has an intensity varying sinusoidally in time with angular frequency ω_a. The normal to the glass plate is at an angle of less than 10° from the incident light beam in order to minimize polarization during reflection. The rest of the light (about 85%) passes through the glass plate (5) and then through a frosted glass to diffuse the light so that the light impinging on the Cartesian-diver rotor is always even in intensity. For purposes of this description, assume the rotor to be moving with constant angular velocity ω_r. (The rotor is made to turn through interaction of eddy currents in the aluminum ring with a pair of alternating-current electromagnets.) The light leaving the Polaroid disk in the rotor (6) has intensity varying sinusoidally in time with frequency $\omega_a - \omega_r$, where $\omega_a \gg \omega_r$. Both light signals are converted into sinusoidally varying voltages 7 and 8 using photocells, which are in turn amplified and filtered (9 and 10) to eliminate high- and low-frequency noise, squared off (11), and fed into a phase difference analyzer which converts the difference in phase

$$\theta = \omega_a t - (\omega_a - \omega_r)t = \omega_r t$$

into a dc voltage (12). This voltage is fed into a strip-chart recorder to give rotor angle θ *vs.* time. (During a retardation time experiment, of course, the output on the recorder will not be the triangular pattern shown in Figure 1 but will be an exponential-like decay curve.) Peak to peak on the sawtooth pattern corresponds to 90° of rotation of the rotor.

More details concerning design of the instrument may be found in Appendix 1.

The ordinary procedure for carrying out an experiment is to set the voltage on the magnets for the desired shear stress, allow the rotor to settle down to its steady-state speed, then manually shut off the magnet power while the rotor motion is recorded. The data obtained from the measurement of the steady-state rotation speed, either on the recorder or visually by timing a number of revolutions of the rotor, allow us to measure the relative viscosity, η_{rel}, simply as

$$\eta_{rel}' = t_r/t_{r_0} = \omega_{r_0}/\omega_r \qquad (1)$$

where t_{r_0} and t_r are the times per revolution of the rotor for the solvent and the solution, respectively, and ω_{r_0} and ω_r are the angular velocities of the rotor for solvent and solution. (The more complicated expression used by Gill and Thompson[2] reduces effectively to eq 1 in this case because of the high rate of rotation (60 rps) of the magnetic field.)

Photographs of a typical recorder tracing for a DNA relaxation experiment may be found in the previous publication.[1]

Theory

The "relaxation time" of a random-coil macromolecule is the interesting quantity. Theory[3,4] predicts that for such a molecule isolated at infinite dilution there are a number of relaxation times, τ_k, given by the formula

$$\tau_k = \frac{M\eta_s[\eta]}{RT}\frac{1}{\nu\lambda_k'\Sigma_k(1/\lambda_k')}, \quad k = 1, 2, \ldots \qquad (2)$$

where M is the molecular weight, η_0 is the solvent viscosity, $[\eta]$ is the intrinsic viscosity, the λ_k' values are eigenvalues of the theory,[4] and ν is a theoretical degeneracy factor. The magnitudes of these eigenvalues depend on the shape of the molecule (*e.g.*, linear, circular, or branched), on the hydro-

* Address correspondence to this author at the Department of Biochemistry and Molecular Biology, Harvard University, Cambridge, Mass. 02138.

(1) R. E. Chapman, Jr., L. C. Klotz, D. S. Thompson, and B. H. Zimm, *Macromolecules*, 2, 637 (1969).

(2) S. J. Gill and D. S. Thompson, *Proc. Nat. Acad. Sci. U. S.*, 57, 562 (1967).

(3) P. E. Rouse, Jr., *J. Chem. Phys.*, 21, 1272 (1953).

(4) B. H. Zimm, *ibid.*, 24, 269 (1956).

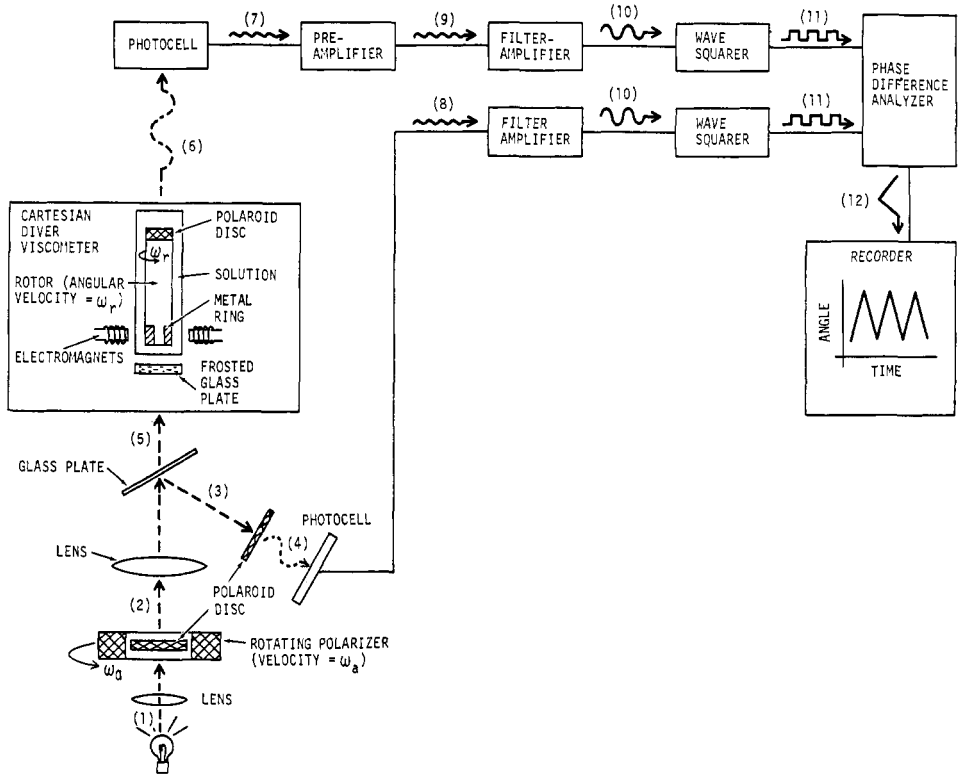

Figure 1. Schematic diagram of apparatus for measuring DNA retardation times. Dashed arrows represent light; solid arrows represent electrical voltage. The shapes of the arrow shafts show either intensity or voltage variation with time. All signal shapes refer to a rotor moving with constant angular velocity. The numbers in parentheses refer to the description in the text.

TABLE I
Calculated[a] Eigenvalues, λ_k', for Linear and Circular Random-Coil Macromolecules

	Linear chains	Circles
λ_1'	5.08	17.07
λ_2'	16.4	50.9
λ_3'	31.5	96.0
λ_4'	49.8	150.4
λ_5'	70.9	212.8
$\nu\Sigma_{i=1}^{\infty}(1/\lambda_i')$	0.438	0.282
$\nu\Sigma_{i=1}^{\infty}(1/\lambda_i')^2$	0.0444	0.00807
$S_1 = \nu\Sigma_{i=1}^{\infty}(\lambda_1'/\lambda_i')$	2.23	4.81
$S_2 = \nu\Sigma_{i=1}^{\infty}(\lambda_1'/\lambda_i')^2$	1.14	2.35

[a] For linear molecules, $\nu = 1$. For circular molecules, $\nu = 2$. These values are calculated for expansion factor $\epsilon = 0.1$. See ref 5 for further details.

dynamic interaction between segments of the molecule, and on excluded-volume effects in the molecule. The eigenvalues for circular and linear random-coil chains calculated by Bloomfield and Zimm[5] are presented in Table I.

Solutions of large DNA molecules show pronounced relaxation effects, as previous authors have shown.[1,6,7] While many of the relaxation times of eq 2 contribute to these effects to some small degree, by far the largest individual contribution is that of k equal to 1. For this reason we were led in our previous work[1] to ignore the other relaxation modes completely. It turns out, however, that the collective effect of the other modes is appreciable, as will be shown below, although this does not change the results of the previous work relating to molecular weight determination.

The molecular theories of viscoelastic behavior of solutions of chain molecules[3,4] naturally lead to expressions for the stress under given conditions of externally applied strain. In our experiments, on the other hand, we measure the strain under given applied stress. Thus, we must invert the theoretical results. This inversion is greatly facilitated by the use of a simple mechanical model to represent the stress–strain behavior of the solution. Of the several possible and equivalent model representations, we have chosen the system of Maxwell elements in parallel (see, for example, Alfrey,[8] chapter A), which is shown in Figure 2. The several Maxwell elements, each consisting of a spring and a dashpot, represent the normal modes of motion of the molecular theory, while a single dashpot represents the viscosity of the solvent, and a lumped inertia, I, represents the mass of the moving system. Since the molecular theory is linear, this model is an exact representation of the theory,[8] except for the minor approximation of lumping all inertias together. In this model the relaxation times, τ_k, are given by

$$\tau_k = \eta_k/K \tag{3}$$

(See caption of Figure 2 for symbols.)

To get an idea of how the various relaxation times interact with each other, first consider a *stress-relaxation* experiment which yields relaxation times directly and in which the relaxation times do not interact. The procedure for performing such an experiment would be to stop the viscometer rotor after the steady-state speed had been attained and to hold the rotor in a fixed position while measuring the stress exerted

(5) V. Bloomfield and B. H. Zimm, *J. Chem. Phys.*, **44**, 315 (1966).
(6) D. S. Thompson and S. J. Gill, *ibid.*, **47**, 5008 (1967).
(7) P. R. Callis and N. Davidson, *Biopolymers*, **8**, 379 (1969).
(8) T. Alfrey, Jr., "Mechanical Behavior of High Polymers," Interscience, New York, N. Y., 1948.

on it by the relaxing DNA molecules. In terms of the model in Figure 2, this procedure would correspond to stopping the mass from moving while the springs, which had been previously stretched by the applied stress, F_0, relaxed against the Maxwell-element dashpot, the solvent dashpot being unable to move. Thus the bar AB in the figure would not move, and each spring would relax independently against its own dashpot.

In a *creep-recovery* process (corresponding to the actual experiments), however, the viscometer rotor is allowed to move under the influence of the relaxing DNA after the initial stress is removed. In terms of the model in Figure 2, the mass and the bar $\overline{AB}$ move, so the relaxation of one Maxwell-element will interact with the other Maxwell elements through its effect on the motion of the bar AB. By definition, the characteristic decay times for stress-relaxation experiments are called relaxation times, and those for creep-recovery experiments are called retardation times.[9] Even if there were an absence of interactions among the various retardation times in a creep-recovery experiment, retardation times are still not in general equal to relaxation times. For example, in the case of only one Maxwell element, the spring of that element must relax against both the Maxwell-element dashpot and the solvent dashpot in a creep-recovery experiment, but only against its own dashpot in a stress-relaxation experiment.

Although it has been impossible so far to solve analytically for the rotor motion, $\theta(t)$, as a function of time after the torque has been removed in the N-Maxwell-element model, it is possible to obtain an approximate expression for the longest time exponential decay, denoted by $\exp\{\alpha_1 t\}$, using second-order perturbation theory (see Appendix 2 for the derivation). The result of this calculation is 2.27, which we rewrite here for convenience

$$\alpha_1 = -\frac{1}{\tau_1}\left[1 + \frac{\tau_1}{\nu\sum_{n=1}^{N}\tau_n}(\eta_{rel} - 1) - \left(\frac{\tau_1}{\nu\sum_{n=1}^{N}\tau_n}\right)^2(\eta_{rel} - 1)^2\sum_{n=2}^{N}\frac{\tau_n}{\tau_1 - \tau_n} + \ldots\right] \quad (4)$$

where η_{rel} is the relative viscosity defined as

$$\eta_{rel} = \eta/\eta_s \quad (5)$$

with η the solution viscosity and η_s the solvent viscosity. Another useful definition is the specific viscosity, η_{sp}, given by

$$\eta_{sp} = \eta_{rel} - 1 \quad (6)$$

This expression for α_1 may be simplified.

First, from eq 2, τ_k may be written in terms of the longest relaxation time, τ_1, and the eigenvalues as follows

$$\tau_k = \tau_1(\lambda_1'/\lambda_k') \quad (7)$$

Now using Table I and eq 7 for a linear polymer, we get

$$\frac{\tau_1}{\nu\sum_{n=1}^{N}\tau_n} \approx \frac{\tau_1}{\nu\sum_{n=1}^{\infty}\tau_n} = \frac{1}{\nu\lambda_1'\sum_{n=1}^{\infty}(1/\lambda_n')} = \frac{1}{S_1} = 0.45 \quad (8)$$

where S_1 is defined in the table. Equation 4 with the use of eq 6 becomes

$$\alpha_1 = \frac{-1}{\tau_1}\{1 + 0.45\eta_{sp} - 0.202\eta_{sp}0(1) + \ldots\} \quad (9)$$

(9) J. D. Ferry, "Viscoelastic Properties of Polymers," Wiley, New York, N. Y., 1961.

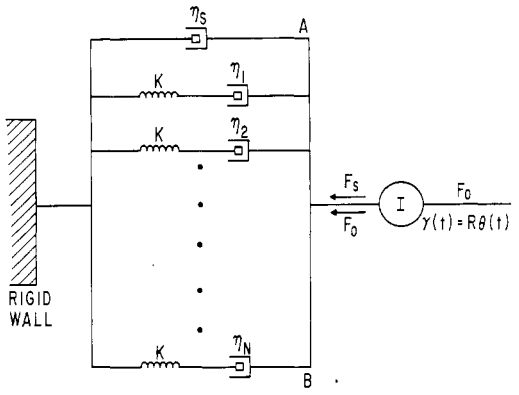

Figure 2. Multi-Maxwell-element model for analyzing the rotor motion during a creep-recovery experiment for a polymer molecule having N relaxation times. η_S is the viscosity coefficient of the solvent, $\eta_1, \eta_2, \ldots, \eta_N$ are the viscosity coefficient increments for each of the normal modes having relaxation times $\tau_k = \eta_k/K$, for $k = 1, 2, \ldots, N$. The circle represents the inertia, I, of the rotor and the surrounding solvent. F_0 is the applied stress on the rotor (from the magnets), F_S is the stress on the rotor due to the solvent alone, and F_D is the stress on the rotor due to the N Maxwell elements. $\gamma(t)$ is the strain along the line of action of the stresses, $\theta(t)$ is the angle of rotation of the rotor and R is the radius of the rotor. The letters A, B refer to a discussion in the text. The model shown is for the non-degenerate case, $\nu = 1$.

where 0(1) denotes terms of order of magnitude unity. Thus for dilute solutions where $\eta_{sp} \ll 1$, the extrapolations to zero concentration should be reasonably linear, and in the limit of zero concentration the relaxation time, τ_1, is obtained exactly. (We should note that any dependence of τ_1 itself on concentration has been ignored in eq 9.)

Another interesting fact about these relaxations may be seen as follows: in the limit of zero concentration the eq 2.16 and 2.17 in Appendix 2 for the motion of the rotor may be solved analytically, yielding

$$\theta(t) = \frac{\omega_r\eta_{sp}}{\sum_n\tau_n}\left[\sum_{k=1}^{N}\tau_k^2(\exp\{-t/\tau_k\} - 1)\right] \quad (10)$$

where $\theta(t)$ is the angular position and ω_r is the angular velocity of the rotor. Thus, the "intensity" of the relaxation of the kth mode is proportional to τ_k^2. Since $\tau_1^2 \gg \tau_2^2 \gg \tau_3^2$ (see Table I), eq 10 says that most of the relaxation intensity (rotor recoil) should be in the longest normal mode. That this is indeed the case is evidenced by the practical linearity at long times of the semilog plot of a typical DNA relaxation presented in Figure 3. Only at very short times can the very small component associated with the faster retardation times be detected.

Besides $[\eta]$ and τ_1, another quantity of interest is the total recoil of the rotor, denoted by Γ_R; Γ_R is defined as the total number of degrees the rotor moves during a relaxation under the opposing influences of the inertia of the system and of the DNA relaxing. Although it has not been possible to solve analytically the complete N-Maxwell-element model as a function of time in all generality, an analytic expression for the total recoil of the rotor in the presence of inertia may be derived. The result of the analytic derivation is eq 2.52 of Appendix 2, namely

$$\Gamma_R = \theta(0) - \theta(\infty) = \frac{\omega_r}{\eta_{rel}}\left[\frac{1}{\delta} - \eta_{sp}\tau_1\frac{S_2}{S_1}\right] \quad (11)$$

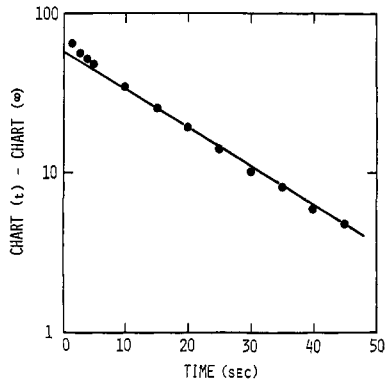

Figure 3. Semilog plot of a T2 DNA relaxation. The data were taken from the average of three recorder tracings similar to that shown in ref 1. The DNA concentration is 14.9 μg/ml, the temperature is 25°, and the shear stress is 0.07 dyn/cm². The solvent is a 75% glycerol–25% aqueous buffer solvent. The ordinate is in arbitrary chart units, which are proportional to rotor angle. See ref 1 for further details.

In this expression

$$\delta = R^2\rho_s/I \tag{12}$$

where R is the radius of the rotor, ρ_s is the frictional coefficient of the solvent dashpot (proportional to η_s), and I is the lumped inertia of the rotors and surrounding solution. Relaxation experiments on pure solvent yield δ directly; see the previous paper[1] for details.

We may note that this expression for Γ_R involves a different combination of the eigenvalues, λ_i', from that found in the equation for the relaxation times, eq 1, and that this combination of eigenvalues in the expression for Γ_R depends on the form of the multi-Maxwell-element model (Figure 2) chosen to represent our creep-recovery experiment, so that measurement of τ_1, η_{rel}, δ, and Γ_R and comparison with eq 11 should test the correctness of the Maxwell-element model. Such measurements on T2 DNA do fit eq 11.

Because the eigenvalues differ for circular chains and linear chains, it was thought that eq 11 might provide a means of distinguishing circular DNA from linear DNA; but unfortunately, for circles the quantity S_2/S_1 equals 0.49 and for linear chains it equals 0.51, so it is impossible in practice to tell circles apart from linear chains through measurement of Γ_R alone.

A creep-recovery experiment performed on a solution containing DNA molecules of many different sizes should yield curved plots when $\log [\theta(t) - \theta(\infty)]$ is plotted against time, the curvature being due to the different retardation times of molecules of different size. (A homogeneous DNA solution gives semilog plots which are effectively linear after an initial transient, as shown in Figure 3.) Thus information about molecular weight distribution is contained in the relaxation curves, and it would be desirable to know how much and what kinds of information about distribution may be extracted from our experiments. Presented below is one possible method of obtaining crude information about molecular weight distribution.

Consider a solution containing concentrations c_i of DNA molecules of molecular weight M_i, where $i = 1, 2, \ldots, P$. Let

$$C = \sum_{i=1}^{P} c_i \tag{13}$$

be the total DNA concentration. Alternatively, in terms of numbers of molecules L_i of size M_i, the total number of molecules L is given by

$$L = \sum_{i=1}^{P} L_i \tag{14}$$

and L_i is related to c_i by

$$L_i = N_a(c_i/M_i) \tag{15}$$

where N_a is Avogadro's number. The motion of the rotor, $\theta(t)$, for this heterogeneous solution is given in the limit of zero concentration and of no inertia by

$$\theta(t) = \frac{\omega_r\eta_{sp}\nu}{S_1\langle\tau_1\rangle}\sum_{i=1}^{P} f_i\tau_{i1}^2 \sum_{k=1}^{N_i}(\lambda_1'/\lambda_k')^2 \times \exp[(\lambda_k'/\lambda_1')(-t/\tau_{i1})] \tag{16}$$

In this equation $f_i = L_i/L$ is the number fraction of molecules of molecular weight M_i, τ_{i1} denotes the longest relaxation time of molecules of component i, $\langle\tau_1\rangle$ denotes the number average of the longest relaxation times τ_{i1} (*i.e.*, $\langle\tau_1\rangle = \Sigma_{i=1}^{P}\tau_{i1}f_i$), and the constant S_1 is defined in Table I. Also, $\theta(\infty)$ has been set equal to zero for convenience. This equation and the one below for the total recoil are derived in Appendix 2.

For the total recoil, Γ_R', which is the limit of Γ_R at zero concentration and no inertia, we have

$$\Gamma_R' = -\omega_r\eta_{sp}\frac{S_2}{S_1}\frac{\langle\tau_1^2\rangle}{\langle\tau_1\rangle} \tag{17}$$

where $\langle\tau_1^2\rangle$ is the number average of the squares of the longest relaxation times. Some information about the distribution of longest relaxatimes (and hence about the molecular weight distribution) is contained in eq 17, specifically, the ratio of the first and second moments, $\langle\tau_1^2\rangle/\langle\tau_1\rangle$.

The amount of total recoil has contributions from each species in the solution. Thus, if the amount of total recoil is compared to the amount of recoil from the longest retardation time of the largest species in solution, denoted by Γ_{11}, a crude estimate of heterogeneity is obtained. Γ_{11} is found experimentally by extrapolating the long-time, straight-line portion of the semilog plots (as in Figure 3) back to zero time and taking the chart-axis intercept (when converted to units of angle) as Γ_{11}. It is easy to derive an expression for Γ_{11} from eq 17 for Γ_R'. The result is

$$\Gamma_{11} = -\frac{\omega_r\eta_{sp}}{S_1\langle\tau_1\rangle}[\nu f_1\tau_{11}^2] \tag{18}$$

(For the definition of ν, see Table I). The ratio Γ_{11}/Γ_R' in the limit of zero concentration can be related to the number fraction of largest molecules, f_1, by

$$\lim_{c\to 0}\left(\frac{\Gamma_{11}}{\Gamma_R'}\right) = 0.85\frac{f_1\tau_{11}^2}{\langle\tau_1^2\rangle}\text{ (for circles)} \qquad 0.88\frac{f_1\tau_{11}^2}{\langle\tau_1^2\rangle}\text{ (for linear chains)} \tag{19}$$

For a homogeneous solution of DNA, Γ_{11}/Γ_R' is 0.85 and 0.88 for circles and linear chains, respectively. For a heterogeneous solution, the ratio would have smaller values. Determination of Γ_{11}/Γ_R' ratios is most useful for estimating heterogeneity when a large amount of homogeneous DNA is mixed with smaller amounts of degradation products of that DNA.

More information about the moments may be obtained as follows. Let

$$A(\beta) = \int_0^\infty t^\beta \theta(t) dt \tag{20}$$

denote "areas" which can be found from the experimental relaxation curves. Now substituting the expression for $\theta(t)$, eq 16, into eq 20 for $A(\beta)$ yields

$$A(\beta) = \omega_r \eta_{sp} \frac{\beta! S_\beta}{S_1} \frac{\langle \tau_1^{\beta+3} \rangle}{\langle \tau_1 \rangle} \tag{21}$$

where $S_\beta = \nu \Sigma_{n=1}^{\infty} (\lambda_1'/\lambda_n')^\beta$, so that the ratios to the mean of successive probability moments, $\langle \tau_1^{\beta+3} \rangle / \langle \tau_1 \rangle$, may be generated by this area method.

It is important to note that the expression for Γ_R and $A(\beta)$ do not yield directly $\langle \tau_1 \rangle$, $\langle \tau_1^2 \rangle$, $\langle \tau_1^3 \rangle$, ..., but only the ratios. Using the experimental data there seems to be no direct method for determining the mean $\langle \tau_1 \rangle$. Nevertheless, it is possible to obtain the mean, variance, etc., if the form of the distribution is assumed *a priori*. To do this in practice, Γ_R', $A(0)$, and A(1) can certainly be measured with sufficient accuracy, so that

$$\frac{A(0)}{\Gamma_R'} = \frac{S_3 \langle \tau_1^3 \rangle}{S_2 \langle \tau_1^2 \rangle} \tag{22}$$

and

$$\frac{A(1)}{\Gamma_R'} = \frac{S_4 \langle \tau_1^4 \rangle}{S_2 \langle \tau_1^2 \rangle} \tag{23}$$

are useful ratios which depend only on the eigenvalues and ratios of the moments of the relaxation time distribution. It is easy to show that for any two-parameter molecular weight distribution—let us say one characterized completely by the mean, m, and standard deviation, σ—one can obtain m and σ from the experimentally determined ratios $\langle \tau_1^3 \rangle / \langle \tau_1^2 \rangle$ and $\langle \tau_1^4 \rangle / \langle \tau_1^2 \rangle$. With very good data, it should even be possible to fit a three- or four-parameter distribution in the above manner.

We note that $\langle \tau_1^3 \rangle / \langle \tau_1^2 \rangle$ is the mean of the distribution of $\tau_i^2 f_i$. This is approximately the distribution of $M_i^3 f_i$, since τ_i^2 varies nearly as M_i^3. Obviously this distribution heavily weights the larger values of M_i.

Finally, there is an interesting formula involving the number of molecules per unit volume which can be derived by combining eq 2 and 11. If we sum eq 2 over the index k, we can show that

$$[\eta] = \frac{RT\nu \Sigma_k \tau_k}{M \eta_s} \tag{24}$$

Analogous to eq 11 we can write

$$\Gamma_1 = -\frac{\omega_r \eta_{sp} \tau_1^2}{\eta_{rel} \Sigma_k \tau_k} \tag{25}$$

where Γ_1 is the part of the recoverable strain associated with the relaxation process of index 1, and inertia has been ignored. We can substitute (24) in (25), uing $\eta_{sp} = [\eta]C$, and introduce the number of molecules per unit volume, L, as

$$L = N_a C / M \tag{26}$$

where N_a is Avogadro's number, to obtain

$$L = -\frac{N_a \eta_s \eta_{rel} \Gamma_1}{RT \omega_r \nu \tau_1^2} \tag{27}$$

The minus sign accounts for the fact that Γ_1 must have opposite sign to ω_r, since it represents motion in the opposite direction. As with eq 2, eq 27 is of uncertain validity at finite concentrations and should be used at infinite dilution only. The number of molecules per unit volume can thus be calculated directly from the viscoelastic measurements alone. Such a relation is, of course, familiar in the theory of rubber elasticity.

Discussion

Our results deviate numerically from those based on the simple model employing only one Maxwell element, which was described in the previous paper,[1] but no qualitatively new features appear. The new results seem to be in better agreement with experiment in that they predict less recoil and less concentration dependence of the first retardation time. A result that is reassuring from the practical standpoint indicates that extrapolations to zero concentration to find the longest relaxation time τ_1 are effectively linear as long as η_{sp} is somewhat less than unity. Furthermore, the shorter time exponential decays contribute so little to the total "intensity" of the relaxation that over most of the course of the latter only the longest process, involving τ_1, is observed. These facts encourage us to believe that measured longest retardation times, extrapolated to zero concentration, should be good measures of the molecular weight through eq 2.

The primary purpose of measuring the relaxation time of a DNA or other macromolecule is to determine the molecular weight and shape. Equation 2 is the basic formula; from this, if the shape is known, the molecular weight can be determined from a measured relaxation time and intrinsic viscosity. If the shape is not known, a serious ambiguity is introduced; for example, the constant involving the eigenvalues differs by about a factor of 2 depending on whether the chains are linear or circular. Another difficulty comes from the differing effects of polydispersity on the intrinsic viscosity and on the relaxation time. The intrinsic viscosity is always an average over all species present. On the other hand, the relaxation time, depending on just how it is determined from the data, reflects more or less the largest species present. In the most interesting cases, where the material consists of one largest molecule (a chromosome) and its breakdown products, measurement of the limiting slope at long times measures the relaxation time of the largest molecule alone. The molecular weight from eq 2 is then fictitiously high.

If the sample is heterogeneous in molecular weight, it is possible to obtain some information about the heterogeneity from the creep-recovery data alone or in combination with viscosity data, as discussed in the preceding section.

Empirical relations are available to relate the molecular weight to the intrinsic viscosity for linear or circular DNA. New empirical relations relating the relaxation times to the molecular weight may be found from these by eliminating the intrinsic viscosity with eq 2. Because of the favorable exponent, these are probably the most accurate means of determining the molecular weight of the largest species in those cases where a distinct largest species is present in considerable amounts.

In the creep-recovery experiment, at least four quantities can be measured, η_{sp}, τ_1, Γ_{11}, and Γ_R'. One might hope to gain much more information from the intercomparison of these than from any one alone. To some extent this is true, though less so than one might expect. If we consider first the case only of a homogeneous chain molecule, either linear or circular, we see that Γ_{11} is 0.85 to 0.88 times Γ_R' in all cases by eq 19, so that the two give essentially equivalent information.

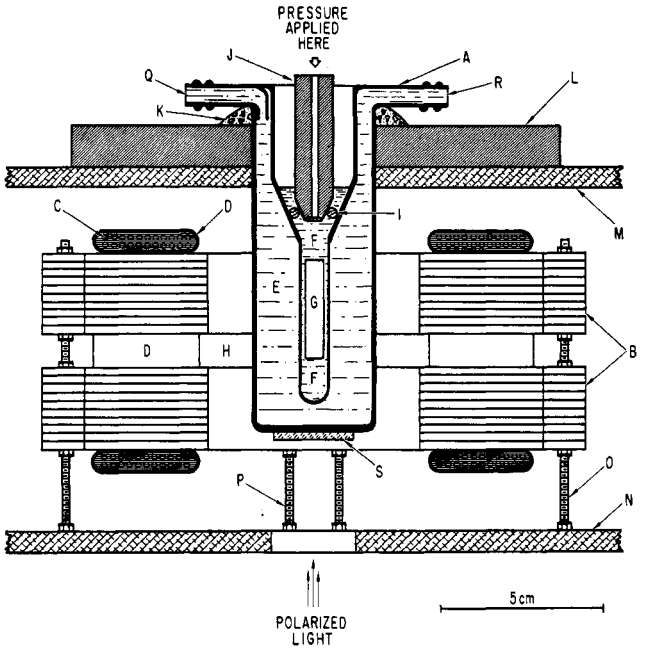

Figure 4. Full-section view of the Cartesian-diver viscometer: (A) the glass thermostated sample chamber (black section lining), (B) electromagnet laminations (horizontal section lining), (C) magnet wire, (D) insulating tape around outside of magnet wire, (E) circulating water, (F) DNA solution, (G) Cartesian-diver rotor (the rotor is shown in outline only; a detailed drawing is presented in Figure 1.2b), (H) air gap in magnets for observing rotor, (I) rubber O ring used to form pressure seal, (J) "pressure bar," (K) plaster, (L) Bakelite block, (M) upper aluminum support plate, (N) middle aluminum support plate (O, P) nuts and bolts for attaching magnet poles to frame, (Q, R) circulating water inlet and outlet, respectively, (*S*) frosted glass plate. All parts are drawn to the scale at the bottom of the figure except the magnet laminations (B) and the magnet wire (C).

Also, we see by eq 11 that the three quantities η_{sp}, τ_1, and Γ_R/ω_R are related so that only two are independent, if one takes M to be known. However, as we have seen in the last section, when the sample is heterogeneous the above relations break down and information about the heterogeneity can be obtained from the extent of the deviations.

A new possibility appears if a sedimentation coefficient is also available. Starting with the well-known Flory–Scheraga–Mandelkern relation, one may use eq 2 to eliminate the intrinsic viscosity. The Flory–Scheraga–Mandelkern[10,11] relation is

$$M^{2/3} = \frac{s[\eta]^{1/3}\eta N_a}{\beta(1 - \bar{v}\rho)} \tag{28}$$

where s is the sedimentation coefficient in Svedberg units, N_a is Avogadro's number, $\bar{v}$ is the partial specific volume of the solute, ρ is the density of the solution, η is the viscosity of the solvent, and β is a constant. Combination with eq 2 yields

$$M = \frac{\kappa N_a (kT)^{1/3}\eta^{2/3}s\tau^{1/3}}{1 - \bar{v}\rho} \tag{29}$$

where κ is a new constant. We use Bloomfield and Zimm's[5] values of the constants for the value of 0.1 for the stiffness parameter, ϵ, appropriate for DNA, to obtain the values of 0.83 and 1.08 for κ for linear chains and for circles, respectively. These values differ by only 30%; thus the molecular weight can be determined within this precision without the necessity of assuming linear or circular chains *a priori*. Comparison of the result with that from eq 2, or with the empirical formulas involving molecular weight and intrinsic viscosity, sedimentation coefficient, or relaxation time should then settle the question of shape. The advantage of using eq 29 with the relaxation time and sedimentation coefficient lies in the ability of both measurements to select the largest species in a heterogeneous mixture of the kind specified above.

Acknowledgment. We gratefully acknowledge technical assistance in the construction of this apparatus by Charles Barna and Philip Chapman. This research was funded by U. S. Public Health Service Grants No. GM 11916 and GM 01045.

Appendix 1. Details of Design of the Instrument

The Optical System. The light source is a General Electric 1133 HI high-intensity 6-V bulb powdered by a Sorensen Q Nobatron (QSB6-4) regulated dc power supply.

The rotating polarizer is turned by a 0.05-hp motor using a large rubber O ring as a belt. The polarizer turns at approximately 800 rpm. The construction of the polarizer is shown in Figure 5. A section view of the Cartesian-diver viscometer, the same in principle as that of Gill and Thompson but differing somewhat in design, is shown in Figure 4. The air gap between the magnet laminations in the figure allows the operator to observe the height and rate of turning of the rotor by means of a small telescope. The mechanism for adjusting the pressure to control the rotor height (not shown in the figure) is the same as that used by Gill and Thompson.[2] The rotor height is maintained constant by means of a servo system. The rotor is centered by lowering it to the rounded bottom of the sample chamber and then raising it to the position desired. A well-constructed rotor will remain centered for 1 hr. Some small details of construction are as follows. The top of the sample chamber (A) and the plaster (K) were painted with dark, waterproof paint to keep out stray light and to prevent erosion of the plaster by spilled liquid. Between the bottom support plate (not shown) and the middle support plate the lenses, rotating Polaroid, etc., are located. The three support plates are bolted together with four 0.5-in. bolts (not shown). The sample chamber diameter is 8 mm. With sample chambers of smaller diameter, there are sometimes problems with small air bubbles or dust in the solution causing the rotor to strike the side of the chamber. For this reason, 8 mm is a minimum size for the sample chamber diameter with 5-mm rotors.

To drive the rotor a pair of alternating-current electromagnets is used. The frame and pole pieces of the electromagnets (see Figure 5a) were constructed from cold-rolled steel sheeting (thickness 0.07 cm) of two different sizes, one size for the poles and another for the frame. The different laminations were stacked alternately and bolted together to a thickness of about 6 cm with a 1-cm air gap in the middle. Each pole piece was wound with about 200 turns of 0.812-mm Formex-coated magnet wire. In Figure 5a the poles of one pair of magnet coils are lettered A and the poles of the other pair are lettered B. One pair generates an eddy current in the metal ring inside the rotor, while the field from the second pair (which is one-third cycle out of phase with that of the first) interacts with the eddy current, causing a torque to be exerted on the rotor. The range 0.2–20 V rms on the two pairs of magnet coils spans the useful shear-stress range.

(10) L. Mandelkern and P. J. Flory, *J. Chem. Phys.*, **20**, 212 (1952).
(11) H. A. Scheraga and L. Mandelkern, *J. Amer. Chem. Soc.*, **75**, 179 (1953).

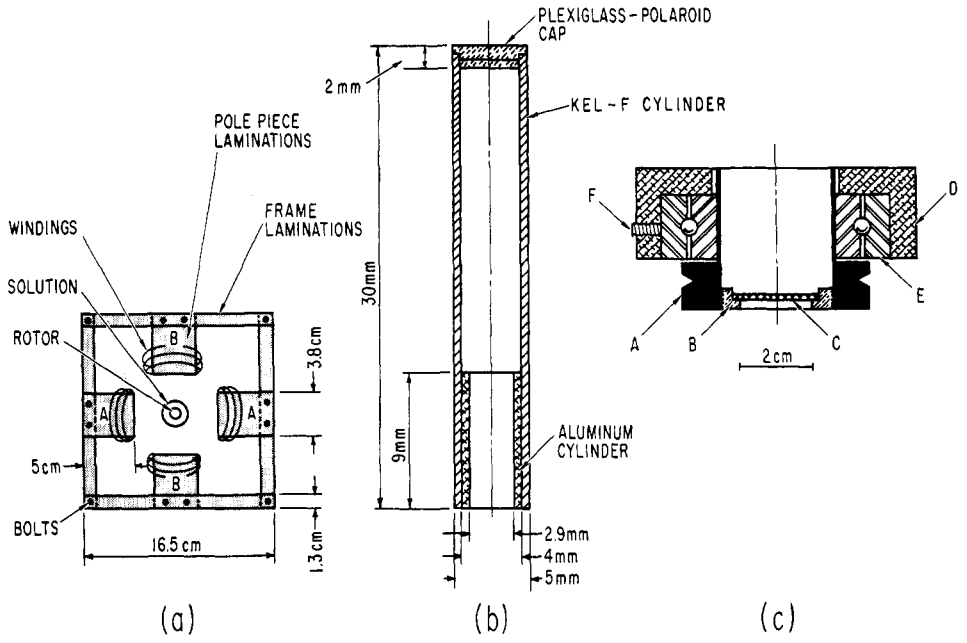

Figure 5. Miscellaneous details of the instrument: (a) top view of the electromagnets (not to scale), (b) a full-section view of the Cartesian-diver rotor (an aluminum cylinder is shown; cylinders of other metals are shorter), (c) a full-section view of the rotating analyzer [(A) aluminum rotator (black section lining), (B) brass mounting ring for Polaroid, (C) Polaroid disk, (D) aluminum frame, (E) ball bearing (Norma 206 PP), (F) set screw to hold ball bearing in frame]. The aluminum rotator is press fitted to the inside of the ball bearing. The V grooves on the side of the rotator are used to seat the O ring connecting it to the driving motor. The drawing is made to scale shown at the bottom of the figure.

Since it is necessary to be able to reproduce exactly the current in each magnet in order to compare solvent rotation times to solution rotation times in the determination of intrinsic viscosity, we measure the voltage with a potentiometer. This circuit and the magnet power supply circuit were shown in the previous publication.[1]

A drawing of the rotor is presented Figure 5b. Since careful construction is necessary in order to get a usable rotor, it is described in detail here.

The Kel-F plastic hollow cylinder is machined from a solid Kel-F rod.

The Polaroid disk is cut from a Plexiglas-laminated Polaroid sheet (thickness, 2 mm). The Polaroid cap is then bonded to the Kel-F cylinder with General Electric LTV-602 clear silicone potting compound.

A metal cylinder of approximately the correct weight is prepared to fit snugly in the end of the rotor. The length of the metal cylinder is adjusted by turning off small amounts of metal from the ends of the cylinder until the assembled rotor just floats in a beaker of water (or solvent in which the rotor is to be used). Then the rotor is further tested by varying the pressure in the Cartesian-diver viscometer to make sure the rotor moves up and down easily under light pressure. We have used gold, bronze, copper, and aluminum for these cylinders. Aluminum and copper give the greatest torque, but are chemically reactive. Gold has proved to be most satisfactory except when high torque is needed. If aluminum is used, the exposed sections are painted with black rubber laboratory paint (Fisher "Plicote") to prevent aluminum ions from escaping into solution and to minimize reflections of light from the aluminum.

A few general comments concerning the rotor. All machining must be done very carefully in order to preserve the cylyindrical symmetry of the parts; asymmetry causes the rotors to precess. The top end of the rotor must be much lighter in weight than the bottom end; top heaviness favors precession also. The present design with a Plexiglas cap on the top and metal plug in the bottom easily eliminates the top heaviness problem. Although in the past precision nmr glass tubing was used for the body of the rotor in place of Kel-F, these rotors cracked at elevated temperatures and it was difficult to replace the Polaroid disk or aluminum cylinder without breaking the rotor; they also showed a greater tendency to precess. With the Kel-F rotor, however, parts are easily replaced, and the rotor is unbreakable.

In Figure 4 a section view of the pressure bar may be seen. The bar is machined from poly(vinyl chloride) plastic. The Plexiglas window at the bottom end is cemented in place with epoxy resin or silicone rubber. The small hole running the length of the bar is, of course, for the passage of light. The lever arm for exerting pressure (see Gill and Thompson[2]) presses on the top of the pressure bar, and the photocell is mounted in this lever arm directly over the hole in the pressure bar.

Both photocells (see Figure 1) are PIN 5 silicon junction photodetectors (United Detector Technology, Santa Monica, Calif.); for these devices, the current response is linear with light intensity.

A detailed circuit diagram of the electronics summarized in Figure 1 is available from the authors.

Although we have not tried one ourselves, there are commercially available phase meters with amplifiers which may be satisfactory.

The output is recorded on an Esterline Angus Model No. 56015 stripchart recorder with a 0.1-sec full-scale response time and 100-mV full-scale sensitivity. Full scale on the recorder at maximum sensitivity is equivalent to about a 2° rotation of the rotor.

Appendix 2. Theory of the Rotor Motion under Various Circumstances

Multi-Maxwell-Element Model. Second-Order Perturbation Theory. To study the interaction of the normal modes in a creep-recovery experiment, we analyze the multi-Maxwell-

element model in Figure 2 for the inertialess case, $I = 0$. It is reasonable to neglect inertia here because we are interested mainly in the longer time relaxations where the rotor is moving most slowly and the inertial "lag" of the rotor is at a minimum.

The relaxation time τ_k for the kth Maxwell element is given by

$$\tau_k = \eta_k/K \tag{2.1}$$

See the caption of Figure 1 for definition of symbols. The sequence of relaxation times, $\tau_1, \tau_2, \ldots, \tau_N$, must be consistent numerically with eq 2 with the eigenvalues given in Table I. In addition, to agree with the beads-and-springs theory[3,4]

$$[\eta] = A \sum_{k=1}^{N} 1/\lambda_k' \tag{2.2}$$

where A may be treated as a constant for present purposes. Thus the viscosity contribution of the kth Maxwell element, η_k, must be proportional to $1/\lambda_k'$, which is proportional to τ_k, and the spring constant, K, must be the same for all k.

We now obtain the equation of motion of the rotor. Since the Maxwell elements are in parallel, the total stress due to the polymer (*i.e.*, due to the Maxwell elements) is

$$F_D = \sum_{k=1}^{N} F_k \tag{2.3}$$

where F_k is the stress due to the kth Maxwell element (the degeneracy factors ν have been left out of all expressions in this appendix, without loss of generality, to avoid complicating the derivations; they have been reinserted in the equations in the main text where necessary); and similarly the total viscosity increment due to the polymer is

$$\eta_D = \sum_{k=1}^{N} \eta_k \tag{2.4}$$

Now applying Newton's law to the inertialess rotor gives

$$F_S + F_D = F_S + \sum_{k=1}^{N} F_k = 0 \tag{2.5}$$

Since for the solvent dashpot we have by definition

$$F_S = -\eta_S \frac{d\gamma}{dt} = -R\eta_S \frac{d\theta}{dt} \tag{2.6}$$

the force law becomes

$$R\eta_S \frac{d\theta}{dt} = \sum_{k=1}^{N} F_k \tag{2.7}$$

For the kth Maxwell element

$$\frac{d\theta}{dt} = \frac{d\theta_{kK}}{dt} + \frac{d\theta_{kD}}{dt} \tag{2.8}$$

and

$$F_{kK} = F_{kD} \tag{2.9}$$

where the subscripts K and D denote spring and dashpot, respectively. From Hooke's law for the springs

$$d\theta_{kK}/dt = -(1/RK)dF_k/dt \tag{2.10}$$

and from the frictional force equation for dashpots

$$d\theta_{kD}/dt = -(1/R\eta_k)F_k \tag{2.11}$$

Substituting these last two equations into eq 2.8 yields

$$\frac{d\theta}{dt} + \frac{1}{R\eta_k} F_k + \frac{1}{RK}\frac{dF_k}{dt} = 0 \tag{2.12}$$

and then substituting for $d\theta/dt$ in this equation and using eq 2.7 gives us the following differential equations for F_k

$$\frac{dF_k}{dt} = \sum_{n=1}^{N} \left(-\frac{K}{\eta_S} - \delta_{ik}\frac{K}{\eta_k} \right) F_i, \; k = 1, 2, \ldots, N \tag{2.13}$$

where δ_{ik} is the Kronecker delta. Equation 2.13 may be cast into more useful form using eq 2.1 and using

$$\frac{K}{\eta_S} = \frac{K}{\eta_D}\eta_{sp} = \frac{K}{\sum_{n=1}^{N}\eta_n}\eta_{sp} = \frac{\eta_{sp}}{\sum_{n=1}^{N}\tau_n} \tag{2.14}$$

to obtain

$$\frac{dF_k}{dt} = \sum_{i=1}^{N} \left[\frac{\eta_{sp}}{\sum_{n=1}^{N}\tau_n} - \delta_{ik}/\tau_k \right] F_i, \; k = 1, 2, \ldots, N \tag{2.15}$$

The solution of this set of equations for F_k when substituted into the integral of eq 2.7, namely

$$\theta(t) = \frac{1}{R\eta_S}\int_0^t \left(\sum_{n=1}^{N} F_k \right) dt \tag{2.16}$$

gives the rotor motion as a function of time.

To attempt to solve the set of eq 2.15 it is convenient to write the set in matrix notation

$$d\mathbf{F}/dt = \mathbf{AF} \tag{2.17}$$

where $\mathbf{F} = \mathbf{F}(t)$ is the $N + 1$ column vector

$$\mathbf{F} = \begin{bmatrix} F_1 \\ F_2 \\ . \\ . \\ . \\ F_N \end{bmatrix} \tag{2.18}$$

and $\mathbf{A}$ is the $N \times N$ matrix

$$\mathbf{A} = \begin{bmatrix} \left\{\frac{\eta_{sp}}{S}\right\} - \frac{1}{\tau_1} & \left\{\frac{\eta_{sp}}{S}\right\} & \cdots & \left\{\frac{\eta_{sp}}{S}\right\} \\ \left\{\frac{\eta_{sp}}{S}\right\} & \left\{\frac{\eta_{sp}}{S}\right\} - \frac{1}{\tau_2} & \cdots & \left\{\frac{\eta_{sp}}{S}\right\} \\ . & & . & . \\ . & & . & . \\ . & & . & . \\ \left\{\frac{\eta_{sp}}{S}\right\} & \left\{\frac{\eta_{sp}}{S}\right\} & \cdots & \left\{\frac{\eta_{sp}}{S}\right\} - \frac{1}{\tau_N} \end{bmatrix} \tag{2.19}$$

where

$$S = \sum_{n=1}^{N} \tau_n \tag{2.20}$$

Formally, the general solution to eq 2.17 is

$$\mathbf{F}(t) = C_1 \exp\{\alpha_1 t\}\chi_1 + C_2 \exp\{\alpha_2 t\}\chi_2 + \ldots + C_N \exp\{\alpha_N t\}\chi_N \tag{2.21}$$

where α_k and χ_k are the eigenvalues and eigenvectors of $\mathbf{A}$. The scalar constants, C_i, are determined from the initial condition

$$\mathbf{F}(0) = \chi\mathbf{C} \tag{2.22}$$

where χ is the matrix, the columns of which are the eigenvectors χ_k and $\mathbf{C}$ is an $N + 1$ column vector whose components are the coefficients C_i.

It is usually impossible to determine the eigenvalues analytically for an arbitrary $N \times N$ matrix, and this appears to be the case for the matrix **A** also. However, at very low polymer concentrations, where $(\eta_{sp}) \to 0$, the matrix **A** approaches a diagonal matrix. Thus, the matrix **A** becomes a good candidate for perturbation analysis.

In the limit of zero concentration the eigenvalues are just the reciprocals of the individual relaxation times; *i.e.*, $1/\tau_1$, $1/\tau_2$, ..., $1/\tau_N$, so that the relaxations of the several Maxwell elements no longer interact and the longest decay process is governed by the relaxation time, τ_1, alone.

We can now use second-order perturbation theory to approximate the magnitude of the effect of interaction among the several relaxations on τ at low, but experimentally practical, concentrations. Briefly, the results of second-order perturbation theory which we require are outlined below. Let **A** be an $N \times N$ matrix (with elements a_{ij}) of the form

$$\mathbf{A} = \mathbf{A}^0 + \gamma \mathbf{A}^1 \tag{2.23}$$

where $\mathbf{A}^0$ is diagonal, $\mathbf{A}^1$ is any matrix (with elements $a_{ij}{}^1$), and γ is a small perturbation. Let α_k denote (the unknown) eigenvalues of **A** and let $\alpha_k{}^0$ denote the eigenvalues of $\mathbf{A}^0$ (*i.e.*, the diagonal elements of $\mathbf{A}^0$). Then

$$\alpha_k = \alpha_k{}^0 + \gamma\alpha_k{}' + \gamma^2\alpha_k{}'' + \ldots \tag{2.24}$$

where

$$\alpha_k{}' = a_{kk}{}^1 \tag{2.25}$$

and

$$\alpha_k{}'' = \sum_{\substack{i=1 \\ i\neq k}}^{N} \frac{a_{ki}{}^1 a_{ik}{}^1}{\alpha_k{}^0 - \alpha_i{}^0} \tag{2.26}$$

With $\gamma = \eta_{sp}$ as the perturbation and with the obvious substitutions from the matrix **A** (eq 2.19) into eq 2.24, we get

$$\alpha_1 = -\frac{1}{\tau_1}\left\{1 + \frac{\tau_1}{S}\eta_{sp} - \left(\frac{\tau_1}{S}\right)\eta_{sp}{}^2 \sum_{i=2} \frac{\tau_1}{\tau_1 - \tau_i} + \ldots\right\} \tag{2.27}$$

Multi-Maxwell-Element Model. Total Recoil. To derive analytically an expression for the total recoil, Γ_R, of the rotor during a relaxation experiment, we start again with Newton's law

$$R(F_S + F_D) = I\frac{d^2\theta}{dt^2} \tag{2.28}$$

Using eq 2.6 for F_S, eq 2.3 for F_D, and defining

$$\delta = R^2\eta_S/I \tag{2.29}$$

we get for Newton's law

$$R\eta_S \frac{d^2\theta}{dt^2} + R\eta_S \frac{d\theta}{dt} - \delta \sum_{k=1}^{N} F_k = 0 \tag{2.30}$$

Now, for the kth Maxwell element, eq 2.12 holds, which may be rewritten using eq 2.1 and 2.14 as

$$R\eta_S \frac{d\theta}{dt} + \frac{\sum_n \tau_n}{\eta_{sp}} \frac{dF_k}{dt} + \frac{\sum_n \tau_n}{\tau_k \eta_{sp}} F_k = 0,\ k = 1, 2, \ldots, N \tag{2.31}$$

The set of eq 2.30 and 2.31 is to be solved subject to the initial conditions for creep recovery

$$\begin{aligned} \theta(0) &= 0 \\ (d\theta/dt)_{t=0} &= \omega_r \\ (d^2\theta/dt^2)_{t=0} &= 0 \\ (dF_k/dt)_{t=0} &= 0 \end{aligned} \tag{2.32}$$

and finally from eq 2.31

$$F_k(0) = -R\eta_S\omega_r\eta_{sp}\frac{\tau_k}{\sum_n \tau_n} \tag{2.33}$$

Taking Laplace transforms of the set of eq 2.30 and 2.31, one obtains after rearranging

$$\begin{aligned} R\eta_S s\left[\frac{1}{\delta}s + 1\right]L(\theta) - L(F_1) - L(F_2) - \ldots - L(F_N) &= \frac{I}{R}\omega_r \\ R\eta_S sL(\theta) + \frac{\sum_n \tau_n}{\eta_{sp}}\left[s + \frac{1}{\tau_k}L(F_k)\right] &= -R\eta_S\tau_k\omega_r,\ k = 1, 2, \ldots, N \end{aligned} \tag{2.34}$$

where $L(\theta)$ and $L(F_k)$ denote the Laplace transforms of $\theta(t)$ and $F_k(t)$, respectively, and s is the Laplace transform variable. The algebraic solution to the set of eq 2.34 for $L(\theta)$ may be written in determinant form as

$$L(\theta) = -\frac{\begin{vmatrix} -\frac{1}{\delta} & -1 & -1 & \cdots & -1 \\ \tau_1 & E\left(s + \frac{1}{\tau_1}\right) & 0 & \cdots & 0 \\ \vdots & & & & \vdots \\ \omega_r & & & & 0 \\ \vdots & & & & \vdots \\ \tau_N & 0 & 0 & \cdots & E\left(s + \frac{1}{\tau_N}\right) \end{vmatrix}}{\begin{vmatrix} \left(\frac{1}{\delta}s + 1\right) & -1 & -1 & \cdots & -1 \\ 1 & E\left(s + \frac{1}{\tau_1}\right) & 0 & \cdots & 0 \\ \vdots & & & & \vdots \\ s & & & & 0 \\ \vdots & & & & \vdots \\ 1 & 0 & \cdots & 0 & E\left(s + \frac{1}{\tau_N}\right) \end{vmatrix}} \tag{2.35}$$

where

$$E = \left(\sum_n \tau_n\right)/\eta_{sp} \tag{2.36}$$

Thus $L(\theta)$ is of the form

$$L(\theta) = \frac{-\omega_r}{s}\frac{R_N(s)}{Q_N(s)} \tag{2.37}$$

where $Q_N(s)$ is an $N + 1$ degree polynomial in s, as can be seen from the diagonal terms, and $R_N(s)$ is Nth degree in s; specifically

$$Q_N(s) = q_{N+1}s^{N+1} + q_N s^N + \ldots + q_0 \tag{2.38}$$

and

$$R_N(s) = r_N s^N + r_{N-1}s^{N-1} + \ldots + r_0 \tag{2.39}$$

Now let $a_1, a_2, a_3, \ldots, a_{N+1}$ be the roots of $Q_N(s)$, then

$$Q_N(s) = Q_N(0) \prod_{i=1}^{N+1} \left(\frac{s}{a_i} - 1\right) = q_0 \frac{1}{\prod_{i=1}^{N+1} a_i} \prod_{i=1}^{N+1} (s - a_i) \tag{2.40}$$

and

$$L(\theta) = -\omega_r \left\{\frac{(\Pi a_i) R_N(s)}{q_0 s(s - a_i)\ldots(s - a_{N+1})}\right\} \tag{2.41}$$

With partial fractions this last equation becomes

$$L(\theta) = \frac{-\omega_r(\Pi a_i)}{q_0} \left\{\frac{D_1}{s} + \frac{D_2}{s - a_1} + \ldots + \frac{D_{N+2}}{s - a_{N+1}}\right\} \tag{2.42}$$

where D_i may be evaluated from the identity

$$\frac{R_N(s)}{s(s - a_1)\ldots(s - a_{N+1})} \equiv \frac{D_1}{s} + \frac{D_2}{s - a_1} + \ldots + \frac{D_{N+2}}{s - a_{N+1}} \tag{2.43}$$

which may be rewritten as

$$R_N(s) \equiv \frac{\Pi a_i}{q_0} Q_N(s) D_1 + s(s - a_2)\ldots(s - a_{N+1})D_2 + \ldots + s(s - a_1)\ldots(s - a_N)D_{N+2} \tag{2.44}$$

Upon inverting the Laplace transform, eq 2.42, one gets

$$\theta(t) = \frac{-\omega_r(\Pi a_i)}{q_0} \{D_1 + D_2 \exp\{a_1 t\} + \ldots + D_{N+2} \exp\{a_{N+1} t\}\} \tag{2.45}$$

We assume now that the physics of the problem guarantees that the a_i's are all real and negative so that from the last equation the total response, $\Gamma_R = \theta(\infty) - \theta(0)$, is given by

$$\Gamma_R = \theta(\infty) = -D_1 \omega_r \frac{\Pi a_i}{q_0} \tag{2.46}$$

since our intial condition is $\theta(0) = 0$. At first glance the condition $\theta(0) = 0$ appears to be inconsistent with $\theta(0) = D_1 + D_2 + D_3 + \ldots + D_{N+2}$ from eq 2.45, but looking at the coefficients of the s^{N+1} term in the identity 2.44 one can see that $D_1 + D_2 + D_3 + \ldots + D_{N+2} = 0$. From the identity 2.44 it is seen that the coefficient D_1 is given by

$$D_1 = r_0/\Pi a_i \tag{2.47}$$

so that putting this into eq 2.46 gives

$$\Gamma_R = -\omega_r(r_0/q_0) \tag{2.48}$$

Thus, to evaluate the total recoil, Γ_R, we need to know only the constant terms q_0 and r_0 of $Q_N(s)$ and $R_N(s)$, respectively. These may be obtained by systematic reduction of the determinants for $Q_N(s)$ and $R_N(s)$ defined in eq 2.35 and 2.37 by the method of minors. This reduction is most easily carried out beginning by taking minors of the last row of $Q_N(s)$ and $R_N(s)$ and proceeding with the lengthy reduction from there. The results are

$$q_0 = E^{N-1} \left\{\frac{\eta_{rel} \sum_i \tau_i}{\eta_{sp} \Pi \tau_i}\right\} \tag{2.49}$$

$$r_0 = E^{N-1} \left\{\frac{-\frac{1}{\delta} \sum_i \tau_i + \eta_{sp} \sum_i \tau_i^2}{\eta_{sp} \prod_i \tau_i}\right\} \tag{2.50}$$

so that finally the total recoil is given by

$$\Gamma_R = \frac{\omega_r}{\eta_{rel}} \left\{\frac{1}{\delta} - \eta_{sp} \frac{\sum_i \tau_i^2}{\sum_i \tau_i}\right\} \tag{2.51}$$

or, using eq 7 to express Γ_R in terms of the longest relaxation time, we get

$$\Gamma_R = \frac{\omega_r}{\eta_{rel}} \left\{\frac{1}{\delta} - \eta_{sp} \tau_1 \frac{S_2}{S_1}\right\} \tag{2.52}$$

Multi-Maxwell-Element Model. Heterogeneous Case. Here we are considering a mixture of molecules of P different sizes. The mechanical model is similar to that pictured in Figure 2, except that there are many more Maxwell elements, one for each relaxation time of each different molecular component. In what follows, let the double subscript, ik, denote the ith component and its kth relaxation time, the component subscript always appearing first and its relaxation time subscript last. For the case of no inertia, Newton's law gives

$$R\eta_S \frac{d\theta}{dt} - \sum_{i=1}^{P} \sum_{k=1}^{N_k} F_{ik} = 0 \tag{2.53}$$

and for the ikth Maxwell element

$$R\eta_S \frac{d\theta}{dt} + \frac{\eta_S}{\eta_{ik}} F_{ik} + \frac{\eta_S}{K_i} \frac{dF_{ik}}{dt} = 0 \tag{2.54}$$

where F_{ik} is the force from the kth normal mode of the ith component, etc.

To cast this last equation in terms of experimentally observable quantities, the following easily verified relationships are of use. First, the relaxation time for the kth normal mode of the ith component is, from eq 2

$$\tau_{ik} = M_i[\eta]_i \eta_S / RTS_1 \tag{2.55}$$

It can be shown that the viscosity coefficient of the kth normal mode of the ith species, η_{ik}, is

$$\eta_{ik} = \eta_S c_i [\eta]_i / S_1 \tag{2.56}$$

where $[\eta]_i$ is the intrinsic viscosity of a solution of homogeneous polymer of molecular weight M_i. Note that η_{ik} must be proportional to $1/\lambda_k'$ in order for consistency with the molecular theory to be maintained. Let

$$\tau_{ik} = \eta_{ik}/K_i \tag{2.57}$$

be the relaxation time of the ikth Maxwell element in the mechanical model, so that using eq 13 and 2.56 in eq 2.57 gives for K_i, the spring constant of the ith component

$$K_i = RT(c_i/M_i) \tag{2.58}$$

Since the number of molecules of component i per unit volume is

$$L_i = N_a(c_i/M_i) \tag{2.59}$$

where N_a is Avogadro's number, we can also write

$$K_i = (RT/N_a)L_i \tag{2.60}$$

To show that these definitions for η_{ik}, τ_k, and K_i are consistent with the expected steady-state behavior of the Maxwell element model, let η_D be the total viscosity increment due to the polymer. Then the identity

$$\eta_S + \eta_D = \eta_S \eta_{rel} \tag{2.61}$$

holds. Now

$$\eta_D = \sum_{i=1}^{P} \sum_{k=1}^{N_i} \eta_{ik} \tag{2.62}$$

that is, the total viscosity increment due to the DNA is a sum over all normal modes $k = 1, 2, \ldots, N_i$ and all components $i = 1, \ldots, P$. Substituting eq 2.56 into 2.62, we get

$$\eta_D = \eta_S \sum_{i=1}^{P} c_i[\eta]_i = \eta_S \sum_{i=1}^{P} (\eta_{sp})_i = \eta_S \eta_{sp} \tag{2.63}$$

so that the definition of η_{ik}, eq 2.56, is consistent both with the molecular theory and with the expected macroscopic behavior of the Maxwell-element model.

Equation 2.54 may now be put in terms of observable quantities. First

$$\frac{\eta_S}{\eta_{ik}} = \frac{\eta_D}{\eta_{sp}\eta_{ik}} = \frac{\sum_{m=1}^{P} \sum_{n=1}^{N_m} \eta_{mn}}{\eta_{sp}\eta_{ik}} \tag{2.64}$$

Equation 2.58 may be written

$$K_i = \frac{c_i}{M_i} \frac{M_m}{c_m} K_m \tag{2.65}$$

so that dividing both numerator and denominator of eq 2.64 by K_i and using eq 2.57 and 7 gives

$$\frac{\eta_S}{\eta_{ik}} = \frac{S_1 \sum_{m=1}^{P} L_m \tau_{m1}}{\eta_{sp} L_i \tau_{ik}} \tag{2.66}$$

Similarly

$$\frac{\eta_S}{K_i} = \frac{S_1 \sum_{m=1}^{P} L_m \tau_{m1}}{\eta_{sp} L_i} \tag{2.67}$$

First substituting eq 2.53 into eq 2.54 to obtain an equation for the F_{ik} alone, one gets

$$\frac{dF_{ik}}{dt} = -\frac{K_i}{\eta_S} \left\{ \sum_{m=1}^{P} \sum_{n=1}^{N_m} \left[1 + \delta_{ik,mn} \frac{\eta_S}{\eta_{ik}} \right] F_{mn} \right. \tag{2.68}$$

and finally substituting eq 2.66 and 2.67 into eq 2.68

$$\frac{dF_{ik}}{dt} = -\sum_{m=1}^{P} \sum_{n=1}^{N_m} \left(\frac{\eta_{sp} L_i}{S_1 \sum_{j=1}^{P} L_j \tau_{j1}} + \frac{\delta_{ik,mn}}{\tau_{ik}} \right) F_{mn} \tag{2.69}$$

which in the limit of very low concentration becomes

$$\frac{dF_{ik}}{dt} = -\frac{1}{\tau_{ik}} F_{ik} \tag{2.70}$$

The solution to eq 2.70 is

$$F_{ik}(t) = F_{ik}(0) \exp\{-t/\tau_{ik}\} \tag{2.71}$$

where $F_{ik}(0)$ is found from substituting the initial conditions $(d\theta/dt)_0 = \omega_r$ and $(dF_{ik}/dt)_0 = 0$ into eq 2.54 to give

$$F_{ik}(0) = -R\eta_S\omega_r \frac{\eta_{ik}}{\eta_S} = \frac{-R\eta_S\omega_r\eta_{sp} L_i \tau_{ik}}{S_1 \sum_{j=1}^{P} L_j \tau_{j1}} \tag{2.72}$$

Finally, putting the expression for $F_{ik}(t)$, eq 2.71, into the integral of eq 2.54 yields for the rotor motion

$$\theta(t) = \frac{\omega_r \eta_{sp}}{S_1 \sum_{j=1}^{P} L_j \tau_{j1}} \left[\left(\sum_{m=1}^{P} \sum_{n=1}^{N_m} L_m \tau_{mn}^2 \exp\{-t/\tau_{mn}\} \right) - \sum_{m=1}^{P} \sum_{n=1}^{L_m} L_m \tau_{mn}^2 \right] \tag{2.73}$$

and for the total recoil

$$\Gamma_R' = \theta(0) - \theta(\infty) = -\omega_r \eta_{sp} \frac{S_2}{S_1} \frac{\langle \tau_1^2 \rangle}{\langle \tau_1 \rangle} \tag{2.74}$$

where eq 7 was used to express τ_{mn} in terms of τ_{m1}. This equation is valid only at very low concentration, in view of the simplification of eq 2.69 into eq 2.70.